Processing and Application of Ceramics 7 [3] (2013) 135–141
DOI: 10.2298/PAC1303135B

Structure and dielectric properties of bismuth sodium titanate ceramic prepared by auto-combustion technique

Tanmaya Badapanda[1], Senthil Venkatesan[2], Simanchalo Panigrahi[2], Pawan Kumar[3]

[1]*Department of Physics, C.V. Raman College of Engineering, Bhubaneswar – 752054, India*
[2]*Department of Physics, Karpagam Institute of Technology, Coimbatore – 641105, India*
[3]*Department of Physics, National Institute of Technology, Rourkela – 769008, India*

Received 12 April 2013; received in revised form 23 September 2013; accepted 24 September 2013

Abstract

$(Bi_{0.5}Na_{0.5})TiO_3$ ceramic was prepared by dry auto-combustion method using urea as a fuel. It was shown that the phase composition of the synthesized powder depends on the amount of urea. The X-ray diffraction study confirmed that single phase rhombohedral structure with space group R3C was obtained in the powder calcined at 700 °C when 25 wt.% of urea was added, but secondary phases were observed with higher addition of urea. Pellets have been formed from the single phase powder and sintered at 1100 °C for 2 and 3 hours. The effect of sintering conditions on the structural and dielectric behaviour was studied in detail. The scanning electron micrographs of pellets showed dense structure with well-defined rectangular grains having larger size after longer sintering time. The temperature and frequency dependence dielectric study of the sintered samples showed two dielectric peaks attributed to the factors caused by the phase transitions from ferroelectric to antiferroelectric and antiferroelectric to paraelectric phase. The dielectric constant and the diffuse phase transition behaviour increases with increase in sintering time.

Keywords*: auto-combustion, scanning electron microscope, dielectric properties, diffuse phase transition*

I. Introduction

The perovskite structure materials with general formula ABO_3 have been found to be very useful for solid-state devices for various industrial applications. Among these compounds with ABO_3 type perovskite structure, much attention has been given to lead based materials, mostly $Pb(Zr,Ti)O_3$ (PZT). Lead based materials have been employed in many piezoelectric applications for years. However, it is well known that PZT based ceramics are environmentally burdened materials because of volatilization of toxic PbO during high temperature sintering. Therefore, it is necessary to develop alternate lead-free materials with excellent piezoelectric properties due to environmental concerns with lead in recent years [1–5].

Among the lead free piezoelectric ceramics $BaTiO_3$ or $Bi_{0.5}Na_{0.5}TiO_3$ are expected to replace PZT due to the growing concern with environmental pollution. Compared to the $BaTiO_3$, the BNT ($Bi_{0.5}Na_{0.5}TiO_3$) has received more attention because $BaTiO_3$ has a relatively high sintering temperature.

Bismuth sodium titanate ($Bi_{1/2}Na_{1/2}TiO_3$ or BNT) has been a perovskite ferroelectric discovered by Smolenskii *et al*. [6]. BNT is considered to be an excellent lead-free piezoelectric ceramic candidate with a perovskite structure of rhombohedral symmetry at room temperature [7–9]. It shows strong ferroelectric properties with a relatively high Curie temperature of 320 °C and a large remnant polarization (38 μC/cm) [10–14]. Compared with PZT, BNT possesses high anisotropic electro-mechanical coupling property with the coupling constant K_p = 16.5–25.5 % in plane direction and $K_t \geq 48$ % in thickness direction, high frequency constant $N_t \geq 2550$ Hz·m and lower room temperature dielectric constant around 290–524 [15] that just meet the demand on ultrasonic application. Therefore, BNT-based ceramics show a great prospect not only for environmental protection but also for various applications. However, the major drawback associated with BNT is that it has very poor sinterability

* Corresponding author: tel: + 91 9437306100
fax: + 91 6612462999, e-mail: *badapanda.tanmaya@gmail.com*

which restricts its applications. The presence of intrinsic point defects as well as the loss of volatile compounds occurs when sintered at high temperature [16]. So in order to improve the properties of BNT ceramics it is necessary to reduce the sintering temperature or improve the densification of ceramics. The low sintering temperature is required to maintain the stoichiometry or nominal composition along with the reduction of energy consumption.

Mostly, BNT is prepared by solid state reaction route with conventional sintering for easy synthesis and low cost. To reduce the sintering temperature and improve the densification of ceramics, various sintering techniques have been adapted via non-conventional sintering processes, such as spark plasma sintering, microwave sintering, multi-step sintering, and reactive sintering. However, these sintering techniques have their own limitations. High calcination temperature and repeated grinding are needed for the conventional solid-state method. Hence, a simple method with low sintering temperature and relatively inexpensive feedstock is required for the preparation of high-quality BNT-based lead-free piezoelectric ceramics. Recently, several methods (hydrothermal synthesis [17,18], the stearic acid gel method [19], the citrate method [20] and the mixed oxide method [21]) have been adopted to fabricate lead-free piezoelectric BNT ceramics.

Combustion synthesis (CS) or self-propagating high temperature synthesis (SHS) is an effective, low cost method for synthesis of ceramics. Using combustion-based methods, monophasic nanopowders with homogeneous microstructure can be produced in shorter reaction times or at lower temperatures, compared to other conventional methods like solid-state synthesis or nitrate method. Extensive research carried out in the last few years has emphasized the SHS capabilities for improvement of materials, energy saving and environmental protection. It is an easy and convenient method for the preparation of a variety of advanced ceramics, catalysts and nanomaterials. It was also observed that the conventional solid state SHS being a gasless combustion process typically yield much coarser particles than solution combustion approach. Many types of combustion synthesis exist which differ mainly in the physical state of the reactants in the combustion modality [22–28]. The basic principle of reduction of processing temperature by using fuel is combustion of the used organic compound within a mixture and releasing a heat that can be effectively supplied to the precursors in the mixture. The energy supplied in this way accelerates the chemical reaction between precursors and also reduces the reaction temperature. Fuel and fuel-to-oxidant ratio plays a very important role in determining the properties of the synthesized products like crystallite size, morphology, phases, specific surface area and nature of agglomeration. In this work urea was chosen as the fuel, which acts as a self-catalyst and generates heat. As its melting point is very low ultimately it helps in increasing the reactivity of the samples yielding a good result as compared to the solid state process.

The main objective of this paper is to systematically study the applicability of adding urea as a fuel in preparation of BNT ceramic through dry auto-combustion technique and to lower the calcination temperature. Urea is used as a fuel which yields powders with the low specific surface area and hard agglomerates, owing to the formation of stable polymer intermediates that prevent the dissipation of heat and thereby promoting sintering of the oxides during combustion. Apart from the synthesis process, the effect of sintering conditions on the microstructure and the relative density of BNT ceramic was investigated.

II. Experimental procedure

Stoichiometric amount of precursors (Bi_2O_3, Na_2CO_3, and TiO_2) was taken and ground for 2 h and then ball milled in a laboratory ball milling machine for around 12 h in the acetone medium. Along with the precursors, urea was added as a fuel in different proportions like 25, 50, 75 and 100 wt.%, and ball milled in acetone medium using zirconia balls as a grinding medium, ensuring complete mixing of precursors and urea. After ball milling, the samples were kept in the air until the complete evaporation of acetone. Then the powders were removed from the bottle and ground for around 4 h until the powders became fine enough. The corresponding chemical reaction is presented by the following equation:

$$Na_2CO_3 + Bi_2O_3 + TiO_2 = 4Bi_{1/2}Na_{1/2}TiO_3 + CO_2 \quad (1)$$

The synthesized powder was calcined at different temperatures in a programmable furnace. The phase formation of the calcined powders was confirmed by the X-ray diffractometer using a Philips diffractometer model PW-1830 with Cu-Kα (λ = 01.5418 Å) radiation in a wide range of 2θ ($20 < 2\theta < 70°$). Pellets have been prepared from the single phased powder by adding 2 wt.% of PVA as binder and uniaxial pressing at 200 MPa. The pellets were sintered at 1100 °C for 2 and 3 hours in a programmable furnace. After heat treatment of the samples, the dry weights of the pellets were measured with a digital electronic balance. Following this, the samples were given different identification to avoid any confusion and kept together in a glass beaker containing kerosene. The beaker with samples was kept in desiccator for around 45 minutes in vacuum created by means of a suction pump. When the bubbles from the beaker stopped coming out, the suction pump was switched off and the vacuum was slowly released. The weights of the pellets were measured, by suspending the pellets in the beaker containing kerosene with the help of a bench, and specially designed hanger, to hang the pellets in the kerosene. The measurement was done with a digital electronic balance and the obtained

weight is represented as the suspended weight. After the suspended measurement the pellets were removed from the beaker and dried using a filter paper in order to remove the kerosene from the surface of the pellets. Then the weights of the pellets were taken using the digital electronic balance and interpreted as the soaked weight. The experimental bulk density was measured by using Archimedes principle:

$$BD = D / (W–I) \quad (2)$$

where BD is bulk density, D is the dry weight, W is the soaked weight and I is the suspended weight.

The relative density ρ_r of a BNT disk is given by:

$$\rho_r = \left(\frac{\rho_m}{\rho_t}\right) \cdot 100 \quad (3)$$

where ρ_t and ρ_m are the theoretical density and the measured density, respectively.

The morphology study was done by using scanning electron microscope (JEOL T-330). For electrical measurements, silver electrodes were applied on the opposite disk faces and were heated at 700 °C for 5 min. The frequency (1 kHz–1 MHz) and temperature (30–200 °C) dependent dielectric measurements were carried out using a Hioki LCR meter (model 3532-50) connected to PC.

III. Results and discussion

3.1 Structural study

Figure 1 shows the XRD pattern of the calcined BNT powders with different fuel concentrations at different temperatures. Figure 1a shows that the formation of BNT phase (perovskite structure with rhombohedral symmetry - space group *R3C*) starts at 600 °C, however some impurity phases also appear. The increase of calcination temperature decreases the amount of impurity phases. Thus, the pure perovskite

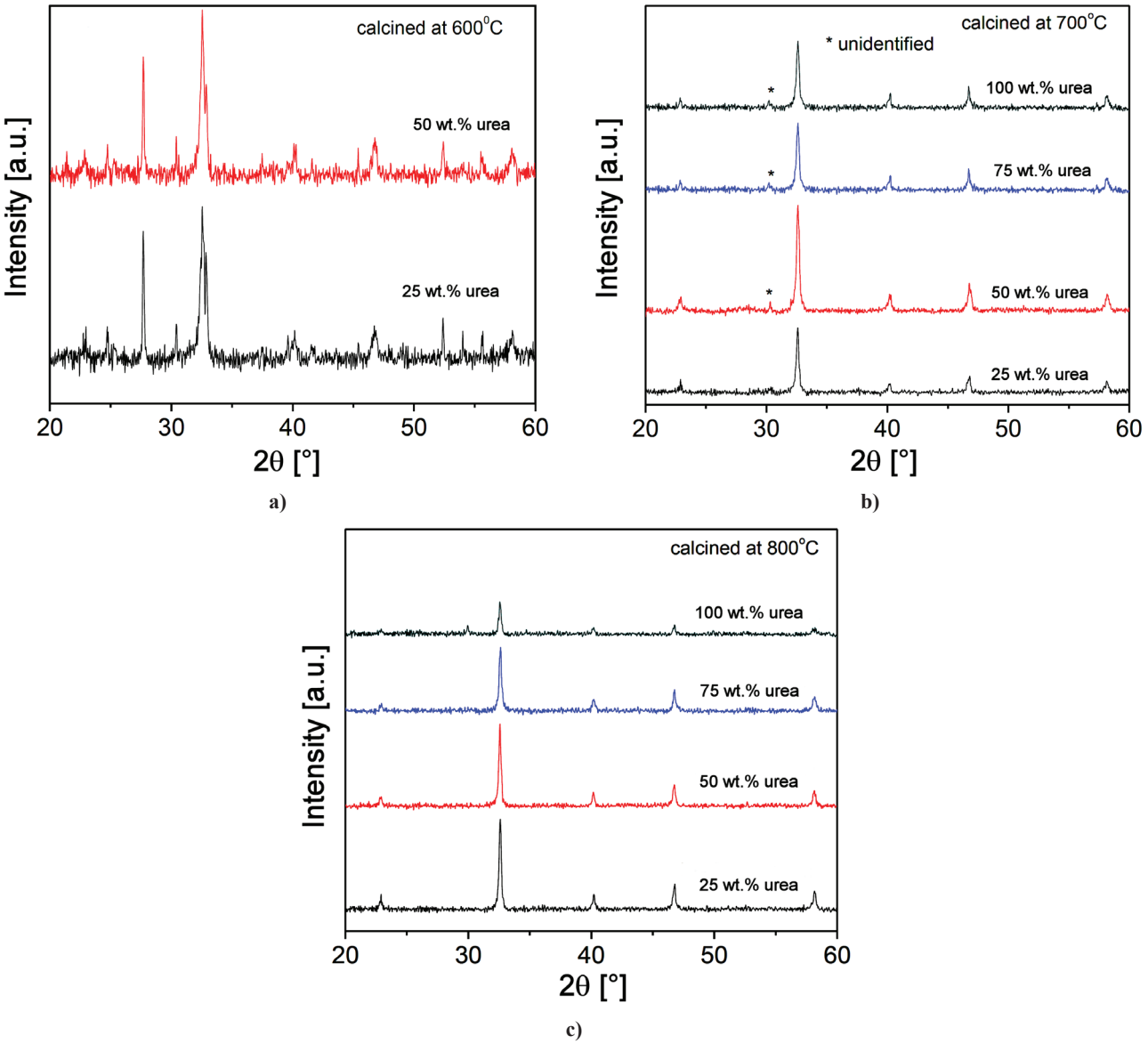

Figure 1. XRD pattern of BNT ceramics with different urea concentrations calcinied at: a) 600 °C, b) 700 °C and c) 800 °C

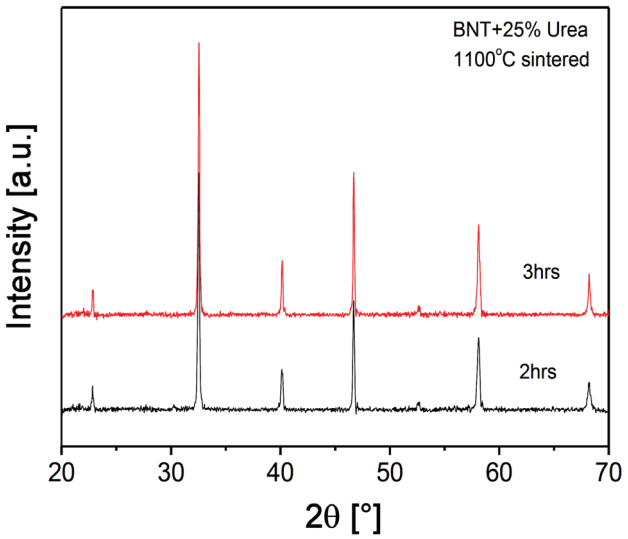

Figure 2. XRD pattern of sintered BNT pellets at 1100 °C for 2 and 3 hours

BNT phase was obtained at 800 °C, and even at 700 °C when the lower fuel concentration (25 wt.% of urea) was used. The reason could be the fact that the uniformity of oxide mixture varies with the variation of urea ratio. All powders calcined at 800 °C have the pure perovskite phase. As our main objective is to reduce the processing temperature of BNT system, we have prepared pellets from the powder synthesized with 25 wt.% urea and calcined at 700 °C. The pellets have been sintered at 1100 °C for different times (2 and 3 hours) to study the effect of sintering condition. Figure 2 shows the XRD pattern of sintered BNT pellets at 1100 °C for 2 and 3 h. The XRD analysis of the sintered pellets shows that the samples (BNT) are single phase. The observed patterns have been indexed using standard pattern JCPDS no. 46-0001. The lattice parameters have been calculated using a computer programme *"CHECKCELL"* and the values are given in Table 1.

3.2 Morphological study

Figure 3 shows the SEM micrograph of the sintered pellets at 1100 °C for different times (2 and 3 hours). The SEM micrographs show the polycrystalline nature of the sample with nearly rectangular grains of different sizes, non-uniformly distributed throughout the sample surface. The grains and grain boundaries are found to be well-defined and clearly visible. The grain size significantly increases by increasing the sintering time. It was found that the average grain size of the sintered BNT ceramics at 1100 °C for 2 and 3 h are ~1.16 and 1.43 μm respectively. The increase in grain size is attributed to the fact that a longer sintering time ensures a larger energy input and facilitates the growth of the grain. Further, during the sintering, the grain grows due to the driving force, which is a reduction in the surface free energy of the consolidated mass of particles. Therefore, the motion of the grain boundary, which minimizes the surface free energy, facilitates the jointing of the BNT grains.

The densities of the sintered ceramics at 1100 °C for different times are about ~93 %TD (percentage of the theoretical density), which is in the similar range of that found by Herabut and Safari [29] (between 93 %TD and 95 %TD) and Nagata and Takenaka [30] (more than 90 %TD).

Table 1. Lattice parameters of BNT ceramic sintered at 1100 °C for 2 and 3 hours

Sintering time [h]	*a* [Å]	*b* [Å]	*c* [Å]	Unit cell volume [Å^3]
2	5.5151 (6)	6.7159(10)	5.5006(5)	176.16
3	5.5289(2)	6.6968(4)	5.5115(3)	176.26

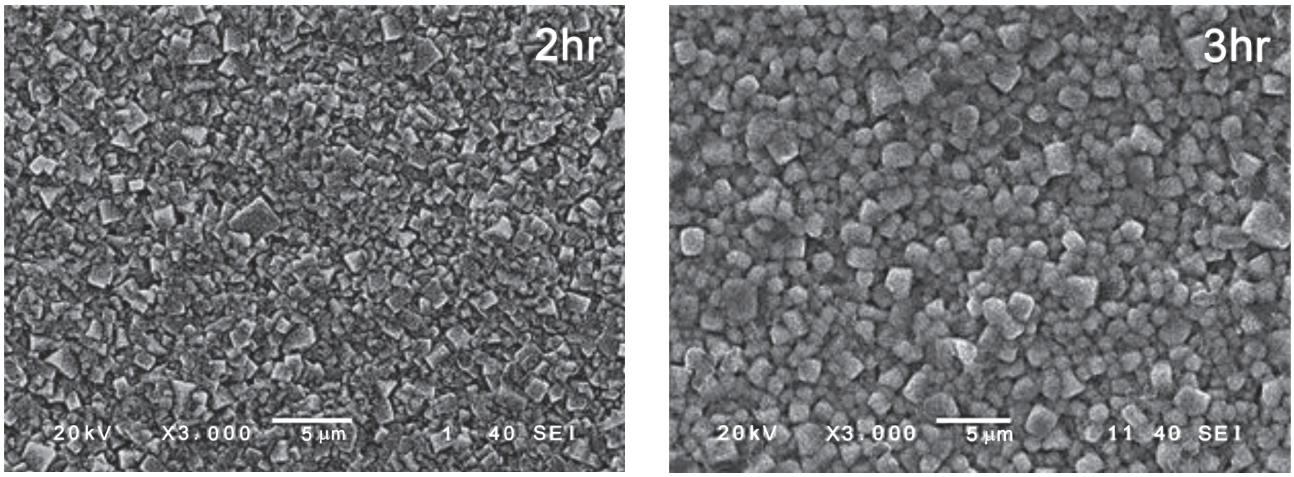

a) **b)**

Figure 3. Scanning electron microscope micrograph of pellets sintered at 1100 °C for different time: a) 2 and b) 3 hours

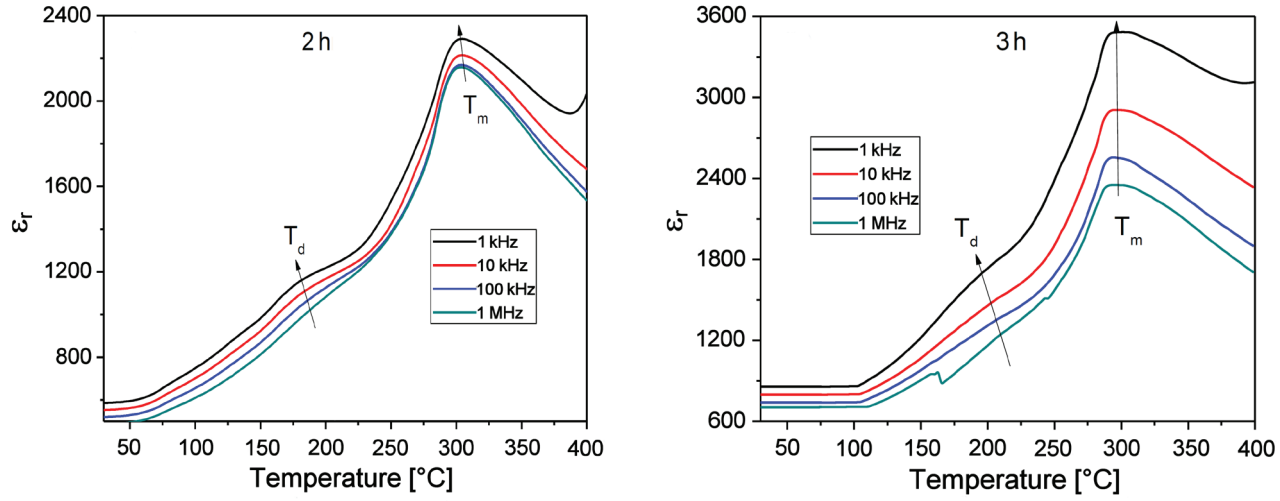

Figure 4. Temperature and frequency dependent dielectric study of BNT ceramics sintered at 1100 °C for: a) 2 and b) 3 hours

3.3 Temperature and frequency dependent dielectric study

The frequency and temperature dependent dielectric behaviour of the BNT ceramic sintered at 1100 °C for 2 and 3 h are shown in Fig. 4. Two characteristic dielectric anomalies were observed in the measuring temperature range - a weak hump and broad dielectric peak. This behaviour is rather analogous to those previously observed in BNT and BNT based ceramics [31–33], with the two dielectric anomalies being referable to a ferroelectric-antiferroelectric transition and a subsequent transition to paraelectric state, respectively. The temperature corresponding to the ferroelectric-antiferroelectric transition is termed as depolarization temperature (T_d) because the specimen is basically depolarized and loses piezoelectric activity above this temperature. The temperature at which the peak value of dielectric constant occurs is named as maximum temperature (T_{max}). Also it is observed from Fig. 4 that temperature T_{max} increases with measuring frequencies whereas the relative dielectric constant decreases as the measuring frequency increases showing evidence of a diffuse phase transition with strong frequency dispersion occurring around the temperature T_{max}.

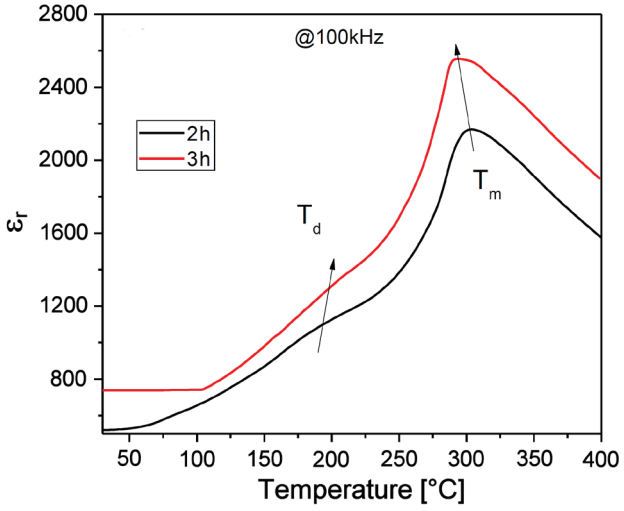

Figure 5. Variation of dielectric constant with sintering temperature and time

Figure 5 shows the variation of dielectric constant of the BNT ceramic sintered at 1100 °C for 2 and 3 hours at frequency of 100 kHz. It is observed that the dielectric constant increases with the increase in sintering time may be due to the better densification and larger grains. Dielectric constant decreases with the increase of frequency for all samples. A more pronounced dispersion of the permittivity values can be observed for the sample sintered for 3 h at 1100 °C. This resembles the behaviour of a relaxor ferroelectric, where the fluctuation of the randomly oriented nanodomains giving rise to the frequency dispersion is suppressed at lower temperatures due to the lack of dynamics [34,35]. The various dielectric data has been presented in the Table 2. The transition temperature is in agreement with the reported values but the dielectric constant is less than that of the BNT ceramic prepared by solid state reaction route [36–38]. The lower dielectric constant is may be due to the smaller grain sizes in comparison to the solid state samples.

The diffusivity (γ) parameter is applied to characterize the relaxor behaviour and it is expressed by a modified Curie-Weiss law [39] given by equation 3:

$$\frac{1}{\varepsilon'} - \frac{1}{\varepsilon'_m} = \frac{(T - T_m)^\gamma}{C} \qquad (4)$$

where γ and C are constant for diffusion factor and the Curie-Weiss constant, respectively. In general, the diffusion factor is between 1 and 2, representing the normal ferroelectric phase transition and completed diffusion phase transition. In the case of $\gamma = 1$, a normal Curie-Weiss law is obtained. The diffusion factor can be employed to describe the diffusion phase transition. The plots of ln $(1/\varepsilon' - 1/\varepsilon'_m)$ as a function of ln $(T - T_m)$ for the BNT samples at frequency of 100 kHz are shown in

Table 2. Parameter obtained from temperature dependent dielectric study at 100 kHz

Sintering time [h]	ε_m	T_d [°C]	T_m [°C]	γ
2	2553	192	303	1.58
3	2162	202	293	1.75

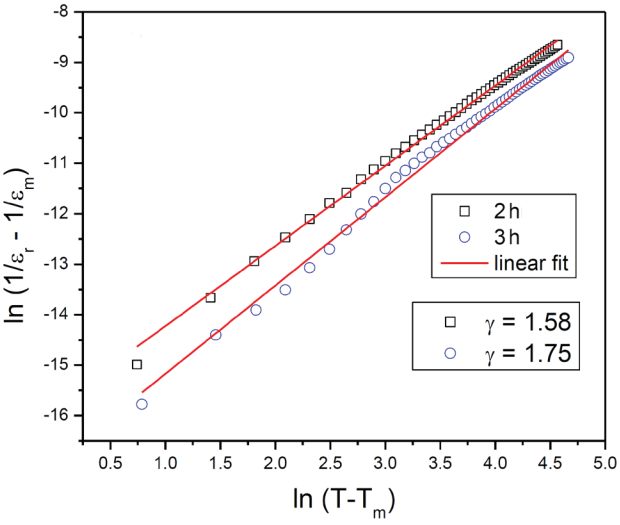

Figure 6. Plot $\ln(1/\varepsilon' - 1/\varepsilon_m)$ vs $\ln(T - T_m)$ of BNT ceramic at 100 kHz

Fig. 6. It is observed that the diffusivity increases with the increase in the sintering time. The diffuse behaviour can be induced by many reasons such as microscopic composition fluctuation, the merging of micropolar regions into macropolar regions, or a coupling of order parameter and local disorder mode through the local strain [40]. Vugmeister and Glinichuk reported that the randomly distributed electrical field or strain field in a mixed oxide system was the main reason leading to the relaxor behaviour [41]. Internal stress occurs to a lesser extent in ceramics with larger grains because of the lower concentration of grain boundaries. So, the decrease in grain size is reasonably considered to be an important factor in changing the delicate balance between the long-range and short-range forces. Therefore, finer grain size and grain boundary effects should be one of the reasons for the appearance of relaxor state.

IV. Conclusions

Lead-free BNT ceramics were synthesized successfully using the auto-combustion route and their structural and dielectric behaviour were investigated. XRD revealed the existence of the pure rhombohedral phase in the powder synthesized with the addition of 25 wt.% urea and calcined at temperature of 700 °C. The BNT ceramic pellets were sintered at 1100 °C for two different times. The scanning electron micrographs of the sintered pellet showed well developed rectangular grains and the increased density of the pellet with the increase in the sintering time. The temperature dependent dielectric study showed that two types of phase transitions occurred in both samples. The dielectric analysis also showed that the transition temperature increases with frequency, thus confirming a diffuse phase transition behaviour. The diffusivity parameter obtained by fitting with the modified Curie-Wises law also increased with the increase in the sintering time.

References

1. J. Yeongho, Y. Juhyun, L. Sangho, "Piezoelectric characteristics of low temperature sintering $Pb(Mn_{1/3}Nb_{2/3})O_3$–$Pb(Ni_{1/3}Nb_{2/3})O_3$–$Pb(Zr_{0.50}Ti_{0.50})O_3$ according to the addition of CuO and Fe_2O_3", *Sens. Actuators A: Phys.*, **135** (2007) 215–219.
2. Y. Zupei, C. Xiaolian, Z. Rui, "Fabrication and electrical characterization of PMN-PZN-PZT ceramic transformers", *Mater. Sci. Eng. B*, **138** (2007) 277–283.
3. P. Marchet, E. Boucher, V. Dorcet, "Dielectric properties of some lead free $Na_{0.5}Bi_{0.5}TiO_3$–$BiScO_3$ and $Na_{0.5}Bi_{0.5}TiO_3$–$BiFeO_3$ ceramics", *J. Eur. Ceram. Soc.*, **26** (2006) 3037–3041.
4. S. Senda, M. Jean-Pierre, "Relaxor behavior of low lead and lead free ferroelectric ceramic of the $(Na_{0.5}Bi_{0.5})TiO_3$–$PbTiO_3$ and $(Na_{0.5}Bi_{0.5})TiO_3$–$(K_{0.5}Bi_{0.5})TiO_3$ systems", *J. Eur. Ceram. Soc.*, **21** (2001) 1333–1336.
5. Q. Xu, X.L. Chen, W. Chen, S.T. Chen , B. Kim, J. Lee, "Synthesis, ferroelectric and piezoelectric properties of some $(Na_{0.5}Bi_{0.5})TiO_3$ system compositions", *Mater. Lett.*, **59** (2005) 2437–2441.
6. G.A. Smolenskii, A. Agranovskaya I, N.N. Krainic, "New ferroelectrics of complex composition IV", *Sov. Phys.-Solid State*, **2** (1961) 2651–2654.
7. T. Takenaka, K. Sakata, "Dielectric, piezoelectric and pyroelectric properties of $(BiNa)_{1/2}TiO_3$-based ceramics", *Ferroelectrics*, **95** (1989) 153–156.
8. T. Takenaka, K. Sakata, K. Toda, "Piezoelectric properties of $(Bi_{1/2}Na_{1/2})TiO_3$-based ceramics", *Ferroelectrics*, **106** (1990) 375–380.
9. H. Nagata, T. Takenakan, "Lead-free piezoelectric ceramics of $(Bi_{1/2}Na_{1/2})TiO_3$–$BiFeO_3$ system", *Key Eng. Mater.*, **169-170** (1999) 37–40.
10. J. Suchanicz, K. Roleder, A. Kania, J. Handerek, "Electrostrictive strain and pyroeffect in the region of phase coexistence in $Na_{0.5}Bi_{0.5}TiO_3$, *Ferroelectrics*, **77** (1988) 107–110.
11. K. Roleder, J. Suchanicz, A. Kania, "Time-dependence of electric permittivity in $Na_{0.5}Bi_{0.5}TiO_3$ single-crystals", *Ferroelectrics*, **89** (1989) 1–5.
12. T. Takenaka, K. Maruyama, K. Sakata, "$(Na_{0.5}Bi_{0.5})TiO_3$–$BaTiO_3$ system for lead free piezoelectric ceramics", *Jpn. J. Appl. Phys.*, **30** (1991) 2236–2239.

13. M.S. Hagiyev, I.H. Ismaizade, A.K. Abiyev, "Pyroelectric properties of $(Bi_{1/2}Na_{1/2})TiO_3$ ceramics", *Ferroelectrics*, **56** (1984) 215–217.
14. S. Said, J.P. Mercurio, "Relaxor behaviour of low lead and lead free ferroelectric ceramics of the $Na_{0.5}Bi_{0.5}TiO_3$–$PbTiO_3$ and $Na_{0.5}Bi_{0.5}TiO_3$–$K_{0.5}Bi_{0.5}TiO_3$ systems", *J. Eur. Ceram. Soc.*, **21** (2001) 1333–1336.
15. X.X. Wang, X.G. Tang, H.L.W. Chan, "Electromechanical and ferroelectric properties of $(Bi_{1/2}Na_{1/2})TiO_3$–$(Bi_{1/2}K_{1/2})TiO_3$– $BaTiO_3$ lead-free piezoelectric ceramics, *Appl. Phy. Lett.,* **85** (2004) 91–93
16. A. Watcharapasorn, S. Jiansirisomboon, T. Tunkasiri, "Sintering of Fe-doped $Bi_{0.5}Na_{0.5}TiO_3$ at < 1000 °C", *Mater. Lett*., **61** (2007) 2986–2989.
17. Y.J. Ma, J.H. Cho, Y.H. Lee, B.I. Kim, "Hydro thermal synthesis of $(Bi_{1/2}Na_{1/2})TiO_3$ piezoelectric ceramics", *Mater. Chem. Phys*., **98** (2006) 5–8.
18. Y.F. Liu, Y.N. Lu, S.H. Dai, "Hydrothermal synthesis of monosized $Bi_{0.5}Na_{0.5}TiO_3$ spherical particles under low alkaline solution concentration", *J. Alloy Compd*.**,** **484** (2009) 801–805.
19. J. Hao, X. Wang, R. Chen, L. Li, "Synthesis of $(Bi_{0.5}Na_{0.5})TiO_3$ nanocrystalline powders by stearic acid gel method", *Mater. Chem. Phys*., **90** (2005) 282–285.
20. Q. Xu, X. Chen, W. Chen, S. Chen, B. Kim, J. Lee, "Synthesis, ferroelectric and piezoelectric properties of some $(Na_{0.5}Bi_{0.5})TiO_3$ system compositions", *Mater. Lett.*, **59** (2005) 2437–2441.
21. D.Z. Jin, X.M. Chen, Z.C. Xu, "Influence of dispersed coarse grains on mechanical and piezoelectric properties in $(Bi_{1/2}Na_{1/2})TiO_3$ ceramics", *Mater. Lett.*, **58** (2004) 1701–1705.
22. K.C Patil, S.T. Aruna, T. Mimani, "Combustion synthesis: an update", *Curr. Opin. Solid State Mater. Sci.*, **6** (2002) 507–512.
23. S.R. Jain, K.C. Adiga, V.R. PaiVerneker, "A new approach to thermochemical calculations of condensed fuel-oxidizer mixtures", *Combust. Flame*, **40** (1981) 71–79.
24. C.C. Hwang, T.H. Huang, J.S. Tsai, C.-S. Lin, C.H. Peng, "Combustion synthesis of nanocrystalline ceria (CeO_2) powders by a dry route", *Mater. Sci. Eng. B*, **132** (2006) 229–238.
25. A.S. Mukasyan, P. Epstein, P. Dinka, "Solution combustion synthesis of nanomaterials", *Proc. Combust. Inst*., **31** (2007) 1789–1795.
26. A.K. Tyagi, S.V. Chavan, R.D. Purohit, "A visit to the fascinating world of nano-ceramics powders via solution-combustion", *Ind. J. Pure Appl. Phys.*, **41** (2006) 113–118.
27. W. Chen, F. Li, J. Yu, "Combustion synthesis and characterization of nanocrystalline CeO_2-based powders via ethylene glycol–nitrate process", *Mater. Lett.*, **60** (2006) 57–62.
28. V. Bedekar, V. Grover, S. Nair, R.D. Purohit, A.K. Tyagi, "Avisit to the fascinating world of nano solution-combustion", *Synth. React. Inorg. Met.-Org. Nano-Met. Chem.*, **37** (2007) 321–326.
29. A. Herabut, A.J. Safari, "Bi-based piezoelectric ceramics", *J. Am. Ceram. Soc*., **80** [11] (1997) 2954–2958.
30. H. Nakada, N. Koizumi, T. Takenaka, "Lead-free piezoelectric ceramics of $(Bi_{1/2}Na_{1/2})TiO_3$–$BiFeO_3$ system", *Key Eng. Mater*., **169-170** (1999) 37–40.
31. I.P. Pronin, P.P. Syrnikov, V.A. Isupov, V.M. Egorov, N.V. Zaitseva, "Peculiarities of phase transition in sodium–bismuth titanate", *Ferroelectrics*, **25** (1980) 395–397.
32. J. Suvhanicz, "Investigations of the phase transitions in $Na_{0.5}Bi_{0.5}TiO_3$", *Ferroelectric*, **172** (1995) 455–458.
33. J. Suchanicz, I.P. Mercurio, P. Marchet, T.V. Kruzina, "Axial pressure influence on dielectric and ferroelectric properties of $Na_{0.5}Bi_{0.5}TiO_3$ ceramics", *Phys. Stat. Sol. (b)*, **225** (2001) 459–466.
34. A.A. Bokov, Z.-G. Ye, "Recent progress in relaxor ferroelectrics and related materials with perovskite structure", *J. Mater. Sci*., **41** (2006) 31–52.
35. L.E. Cross, "Relaxor ferroelectrics", *Ferroelectrics*, **76** (1987) 241–267.
36. T. Oh, M.-H. Kim, "Phase relation and dielectric properties in $(Bi_{1/2}Na_{1/2})_{1-x}Ba_xTiO_3$ lead-free ceramics", *Mater. Sci. Eng. B*, **132** (2006) 239–246.
37. J.H. Cho, S.C. Lee, L. Wang, H-G. Yeo, Y-S. Sung, M-H. Kim, T.K. Song, "Dielectric properties and phase transitions in hetero-valent-ion-substituted $(Bi_{0.5}Na_{0.5})TiO_3$ ceramics", *J. Korean Phys. Soc.*, **56** (2010) 457–461.
38. H.Y. Tian, D.Y. Wanga, D.M. Lin, J.T. Zeng, K.W. Kwok, H.L.W. Chan, "Diffusion phase transition and dielectric characteristics of $Bi_{0.5}Na_{0.5}TiO_3$–$Ba(Hf,Ti)O_3$ lead-free ceramics", *Solid State Commun.*, **142** (2007) 10–14.
39. K. Uchino, S. Nomura, "Critical exponents of the dielectric constants in diffused-phase-transition crystals", *Ferroelectrics*, **44** (1982) 55–61.
40. D. Viehland, M. Wuttig, L.E. Cross, "The glassy behavior of relaxor ferroelectrics", *Ferroelectrics*, **120** (1991) 71–77.
41. B.E. Vugmeister, M.D. Glinichuk, "Dipole glass and ferroelectricity in random-site electric dipole systems", *Rev. Mod. Phys*., **62** (1990) 993–1026.